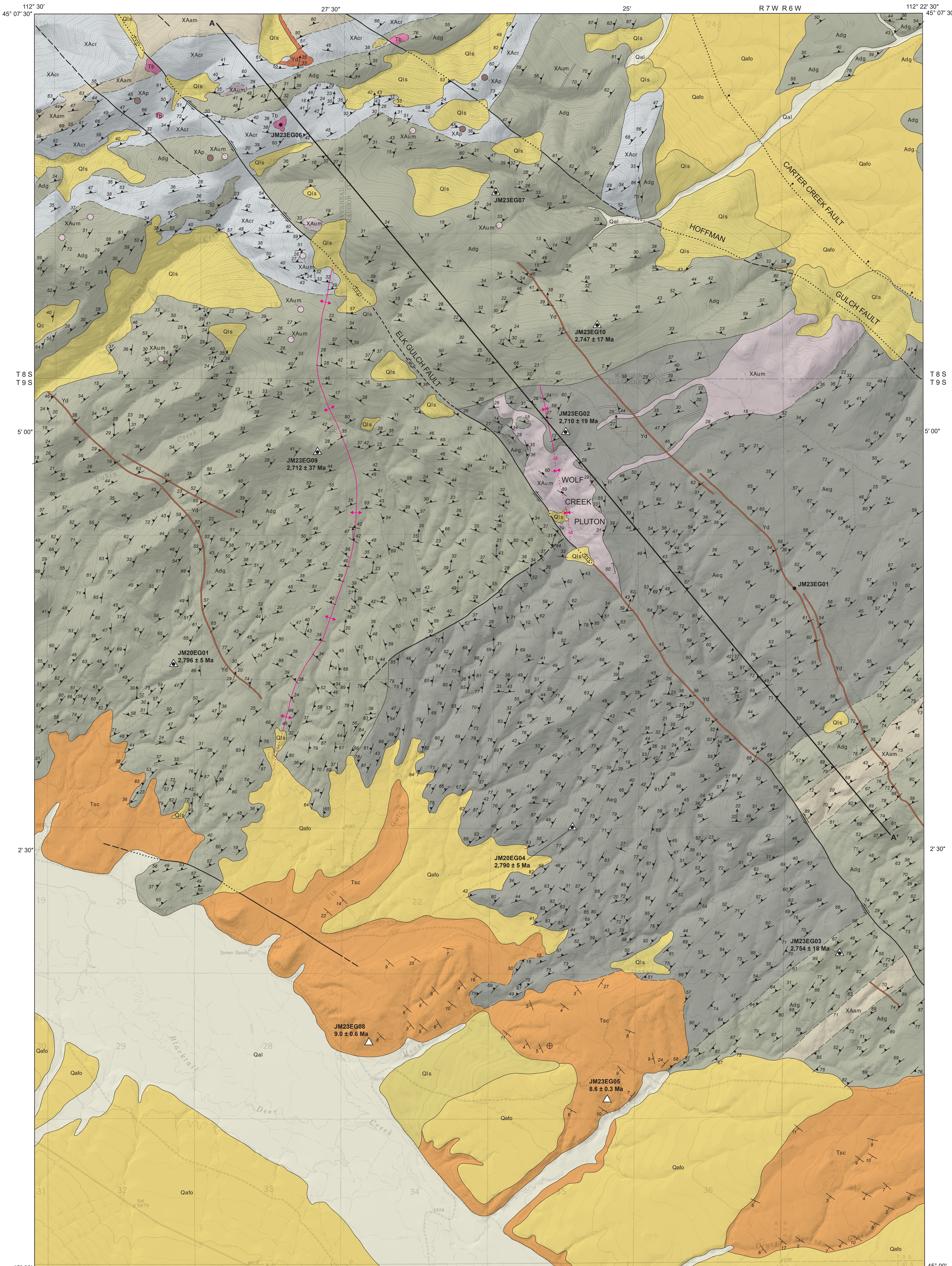

Basemap produced by the United States Geological Survey
Elk Gulch 1:24,000-scale quadrangle map
Control by: USGS and USC&GC
Compiled from aerial photographs taken 1960
Field checked: 1961
Projection: Polyconic
Vertical Datum: National Geodetic Vertical Datum of 1929
Horizontal Datum: 1927 North American Datum

Shaded relief created from 10-meter digital elevation model from U.S. Geological Survey National Elevation Dataset.

SCALE 1:24,000

CONTOUR INTERVAL 40 FEET
NATIONAL GEODETIC VERTICAL DATUM OF 1929

Maps may be obtained from:
Publications Office
Montana Bureau of Mines and Geology
1300 West Park Street
Butte, Montana 59701-8997
Phone: (406) 496-4174
http://mbmg.mtech.edu

CORRELATION CHART

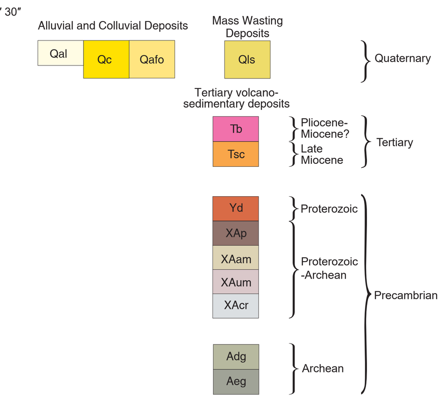

MAP SYMBOLS

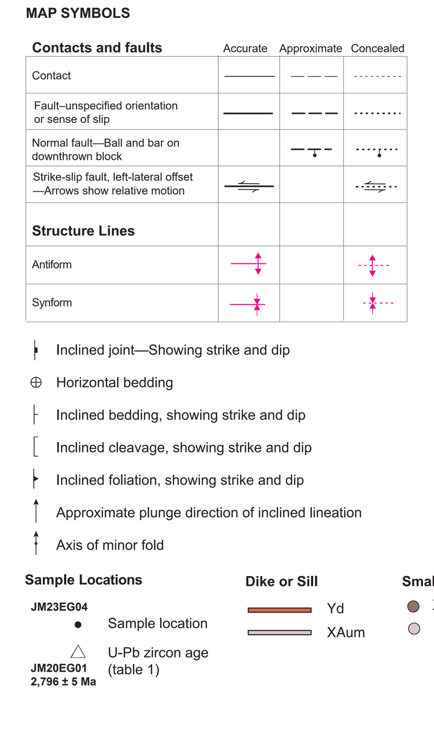

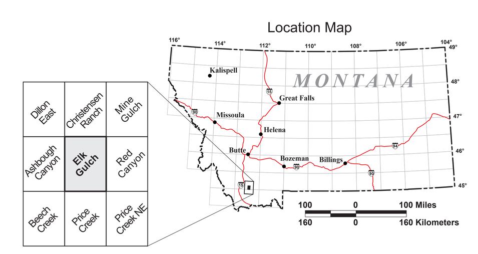

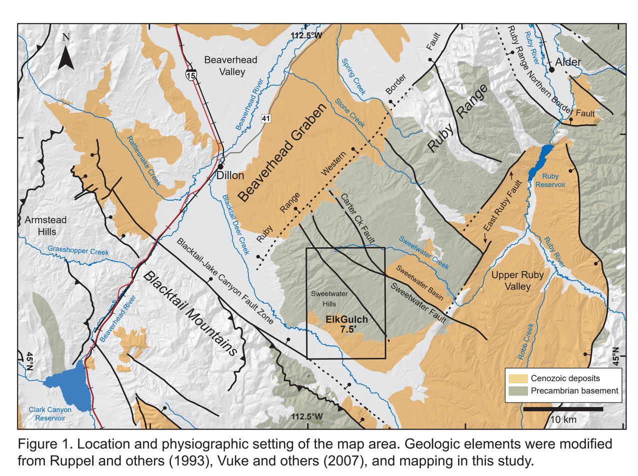

Figure 1. Location and physiographic setting of the map area. Geologic elements were modified from Ruppel and others (1993), Vuke and others (2007), and mapping in this study.

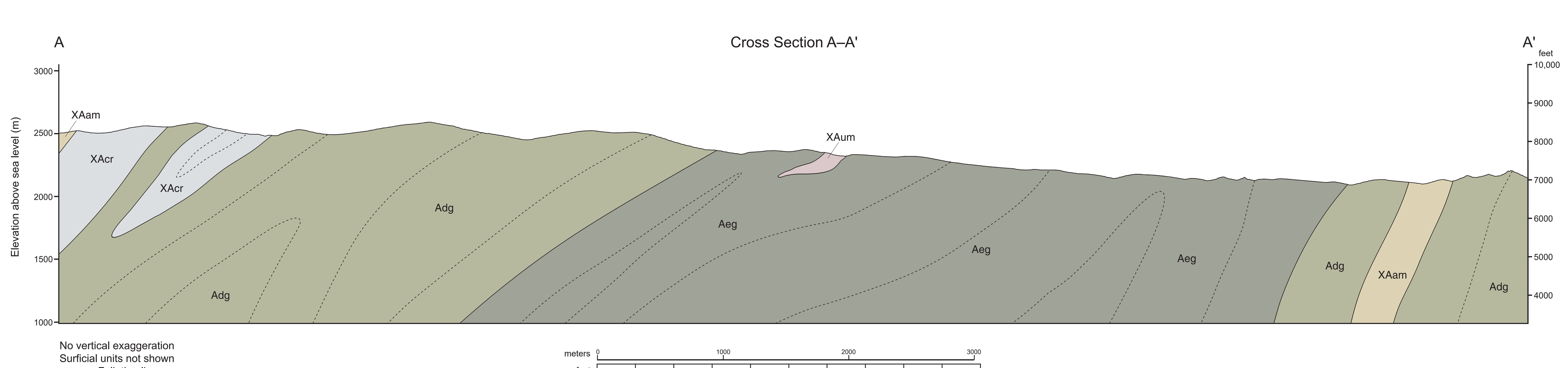

Research supported by the U.S. Geological Survey, National Cooperative Geologic Mapping Program, under USGS award G23AC00457.
GIS production: Jesse Mosolf, Patricia E. Gallagher, and Yiwen Li, MBMG. Map layout: Susan Smith, MBMG. Editing: Susan Barth, MBMG.

LOCATION AND PHYSIOGRAPHIC SETTING

The Elk Gulch 7.5′ quadrangle is in Beaverhead and Madison Counties, approximately 22.5 km (14 mi) southeast of Dillon, Montana, covering parts of the Sweetwater Hills and Blacktail Deer Creek Valley near the southern terminus of the Ruby Range (fig. 1). The Sweetwater Hills are generally underlain by rugged, upland terrain covered by a mix of grassland and sagebrush steppes, with tracts of coniferous woodlands on north-facing slopes. The exposure of the bedrock geology and overlying unconsolidated Cenozoic sedimentary cover is generally good. The Elk Gulch quadrangle spans a drainage divide separating Blacktail Deer and Sweetwater Creeks that flow to the Jefferson River. The quadrangle elevation ranges from 1,765 m (5,790 ft) along Blacktail Deer Creek to 2,588 m (8,490 ft) at Benson Peak.

PREVIOUS MAPPING

The Elk Gulch 7.5′ quadrangle was included in small-scale mapping by Ruppel and others (1993, scale 1:250,000) and Klepper (1950, scale 1:250,000). Large-scale mapping by Okuma (1971, scale 1:24,000) and James (1990, scale 1:24,000) covered the northern part of the quadrangle and was focused on the metamorphic basement rocks. Additional work on the Precambrian basement rocks in the Ruby Range relevant to the geology of this map was conducted by Garihan (1979a, b), Karasevich (1980), Dahl (1979, 1980), Dahl and Friberg (1980), and Desmarais (1981). The region's Cenozoic sedimentary framework is summarized by Thomas and Sears (2020), Vuke (2020), and references therein.

METHODS

Geologic Mapping

Field mapping was conducted over approximately 3.5 months in 2023 for the STATEMAP component of the United States Geological Survey (USGS) National Cooperative Geologic Mapping Program (NCGMP). A 1:24,000-scale topographic base was utilized for field mapping, and geologic contacts were refined by high-resolution satellite imagery (ESRI, 2024) and the USGS 3DEP lidar data. Structure and observational data were located and measured with a traditional hand transit and an Apple iPhone 14. Metamorphic foliations represent all types of recognizable surfaces of metamorphic origin. In gneiss and metasedimentary rocks, the foliation commonly parallels mineral compositional layering. Metamorphic lineations represent mineral alignment, fold axes, and the intersection of foliation planes. Field sheets were scanned and georegistered in GIS software. The geologic data were subsequently digitized to the Geologic Map Schema (GeMS) geodatabase required by the NCGMP.

Whole-Rock Element Chemistry and U-Pb Geochronology

Rock samples for whole-rock geochemistry and U-Pb geochronology were processed at the MBMG mineral separation laboratory. A 100- to 200-g split of the crushed material was prepared for bulk-rock geochemical analysis and analyzed by X-ray fluorescence (XRF) and inductively coupled plasma mass spectrometry (ICP-MS) at the Peter Hooper GeoAnalytical Lab, Washington State University, Pullman. Zircon was isolated from samples by standard density and magnetic separation techniques at the MBMG mineral separation laboratory and analyzed by laser ablation inductively coupled plasma mass spectrometry (LA-ICPMS) at the University of California, Santa Barbara.

Major and trace element data are plotted in figure 2 (Mosolf and others, in review). Table 1 provides U-Pb zircon ages calculated from samples with coherent and interpretable distributions of single-crystal dates, and their respective age distributions are plotted in figure 3. The complete U-Pb zircon datasets and analytical methods are reported in Mosolf and Kylander-Clark (2023) and Brennan and others (in review) .

DESCRIPTION OF THE MAP UNITS

The Elk Gulch geologic map shows rock units exposed at the surface or overlain by a thin surficial cover of soil and colluvium. Surficial sedimentary and mass movement deposits are shown where they are thick and extensive enough to be mapped at 1:24,000 scale. Igneous and metamorphic rocks are classified using the International Union of Geological Sciences nomenclature (Le Bas and Streckeisen, 1991; Schmid and others, 2007). Minerals in igneous and metamorphic rock units are listed in order of decreasing abundance. Grain size classification of unconsolidated and consolidated sediment is based on the Wentworth scale (Lane, 1947). Multiple lithologies within a rock unit are listed in order of decreasing abundance.

Quaternary Deposits

Quaternary alluvial fans (Qafo) onlap the northwestern extent of the Carter Creek fault escarpment, covering the Bozeman Group and Precambrian rocks in the Sweetwater Basin. Large alluvial fans shed from the Blacktail Mountains cover the older Tertiary sedimentary deposits southwest of Blacktail Deer Creek. Landslide deposits (Qls) occur throughout the map area, with several localized along fault traces. Wide alluvial deposits (Qal) have formed along Blacktail Deer Creek, a perennial stream in the map area.

Qal **Alluvium (Quaternary: Holocene)**—Unconsolidated, poorly to well-sorted, weakly stratified gravel, sand, silt, and clay. Clasts are subangular to rounded cobbles and smaller. Thickness is generally less than 6 m (20 ft).

Qc **Colluvium (Quaternary: Holocene and Pleistocene?)**—Unconsolidated slope deposit that contains angular, poorly sorted pebbles, cobbles, and boulders. Includes talus. Thickness is generally less than 10 m (33 ft).

Qafo **Alluvial fan deposit (Quaternary: Holocene and Pleistocene?)**—Unconsolidated, poorly sorted cobbles, gravel, sand, and silt forming extensive, fan-shaped deposits shed from the Carter Creek fault escarpment and Blacktail Mountains. Thickness as much as 30 m (100 ft).

Qls **Landslide deposit (Quaternary: Holocene and Pleistocene?)**—Unstratified, poorly sorted rock fragments deposited by slumps, slides, rock falls, and debris flows. Typically characterized by hummocky topography, subdued landslide scarps, and rock talus. Variable thickness, generally less than 30 m (100 ft).

Tertiary Volcano-Sedimentary Deposits

Tertiary volcano-sedimentary deposits of the Sixmile Creek Formation (Bozeman Group) were mapped along the southern flank of the Sweetwater Hills, unconformably overlying the Archean basement rocks (fig. 4A). The unconsolidated deposits generally consist of roundstone conglomerate and interbedded tephra correlated to the informal Big Hole River and Anderson Ranch members of the Sixmile Creek Formation (see Thomas and Sears, 2020, and references therein). The informal units were challenging to map in the quadrangle and were lumped as an undivided unit (Tsc).

The tephra beds of the Anderson Ranch member erupted from silicic calderas that formed in the wake of the Yellowstone hotspot as it tracked northeastward along the eastern Snake River Plain (Shane and Sears, 1995; Thomas and others, 1995; Perkins and Nash, 2002; Sears and others, 2009). In the Blacktail Deer Creek area outside the quadrangle, Perkins and Nash (2002) correlated tephra beds in the Anderson Ranch member with the 14 Ma Owyhee–Humbolt, 12.5 Ma Bruneau–Jarbidge, 10 Ma Twin Falls–Picabo, and 6–4 Ma Heise volcanic fields (Pierce and Morgan, 1990). Scattered outcroppings of basalt in the northern part of the quadrangle (Tb) are possibly equivalent to the Timber Hill Basalt member (approximately 6 Ma; e.g., Mosolf and Sears, 2024), or a Pliocene basalt northeast of the map area (approximately 4 Ma; Marvin and others, 1974).

Tb **Basalt, undivided (Pliocene?)**—Small, scattered outcroppings (<0.02 km^2, 0.01 mi^2) of aphanitic basalt in the northern part of the quadrangle containing sparse olivine phenocrysts (<1 percent). It is not apparent if the basalt is volcanic or subvolcanic. Thickness unknown.

Tsc **Sixmile Creek Formation, undivided (late to middle Miocene)**—Weakly lithified sequence of conglomerate, sandstone, mudstone, and tephra up to 500 m (1,500 ft) thick. Published radiometric age dates for the Sixmile Creek Formation span 16–3.7 Ma, consistent with vertebrate fossil ages (Monroe, 1976; Fritz and Sears, 1993; Mosolf and Sears, 2024). Maximum depositional U-Pb zircon ages obtained in this study span 9.0–8.6 Ma (table 1; fig. 3). The Sixmile Creek Formation is locally cut by pediments and covered by large alluvial fans (Qafo).

Big Hole River member (Miocene)—Well-sorted, well-rounded fluvial conglomerate that forms crudely channelized bedforms. Conglomerate clasts are typically spherical, pebble to cobble sized, and predominantly composed of quartzite, but also include gneiss, basalt, rhyolite, and limestone. Clast lithologies include vitreous pink quartz-arenite, fine-grained white quartz-arenite, black quartz-arenite, black chert laced with quartz veins, and brown cherty litharenite. Subordinate sandstone beds are cross-bedded and form tabular, stepped cliffs. The Big Hole River member rarely crops out and typically forms gravel-draped hillslopes.

Anderson Ranch member (Miocene)—Distinct white, friable beds of tephra up to 30 m (100 ft) thick that are interlayered with roundstone conglomerate, sandstone, and mudstone. The tephra beds are generally lenticular, trough cross-bedded and composed of a mix of ash and pumice, silicic sand and gravel, and tabular to irregular fragments of tuffaceous rip-up clasts. Tephra beds crop out in the prominent bluffs bordering along Blacktail Deer Creek in the south part of the map area.

Table 1. U-Pb zircon geochronology.

Sample	Lithology	Unit	Latitude (°N)	Longitude (°W)	No. spot analyses[a]	Method	Age (Ma)	2σ	MSWD[b]
JM23EG05	sandstone	Tsc	45.0167	-112.4204	12/120	MDA-LI	8.6	0.3	4.9
JM23EG08	tuffaceous sandstone	Tsc	45.0224	-112.4539	4/200	MDA 206/238	9.0	0.6	9.0
JM23EG02	migmatic gneiss	Aeg	45.0832	-112.4261	7/60	MEA 207/206	2,710	19	0.9
JM23EG09	augen gneiss	Adg	45.0813	-112.4610	5/60	MEA 207/206	2,712	37	2.5
JM23EG10	garnet gneiss	Adg	45.0939	-112.4217	53/60	MEA 207/206	2,747	17	1.2
JM23EG03	garnet gneiss	Adg	45.0313	-112.3877	43/60	MEA 207/206	2,754	18	2.6
JM20EG04	garnet gneiss	Aeg	45.0438	-112.4252	40/40	MEA 207/206	2,790	5	1.0
JM20EG01	quartzofeldspathic gneiss	Adg	45.0601	-112.4813	40/40	MEA 207/206	2,796	5	0.6

Note: [a]Numerator is the number of spots used for age calculation; the denominator is the total number of spots analyzed.
[b]MSWD is the Mean Square Weighted Deviation.
Method: MDA 206/238 max depositional age, weighted mean of youngest ^{206}PB/^{238}U dates.
MDA -LI max depositional age determined by the lower intercept age on a Tera Wasserberg plot.
MEA 207/206 minimum emplacement age determined by weighted mean of oldest ^{207}PB/^{206}Pb dates.
Zircon separates were prepared at MBMG and analyzed by LA-ICPMS at the University of California, Santa Barbara.
Latitudes and longitudes are in the 1984 World Geodetic Survey (WGS84) datum.
See Mosolf and Kylander-Clark (2023) and Brennan and others (in review) for full datasets and interpretations.

Precambrian Metamorphic and Intrusive Rocks

The Ruby Range is divided by three general belts of Precambrian metamorphic rock that young to the west, including the Elk Gulch Suite (Aeg), the Dillon Gneiss (Adg), and the Christensen Ranch Metasedimentary Suite (XAcr). The Elk Gulch Suite is the structurally deepest metamorphic assemblage and is composed of gneiss, migmatite, and amphibolite. Minimum emplacement ages of gneissic intervals span approximately 2.79–2.71 Ga (table 1; fig. 3). The Dillon Gneiss is a complex metamorphic assemblage dominated by massive-to-foliated granitic gneiss that forms the crest of the Ruby Range (fig. 4B). The rocks are generally enriched in incompatible elements with minimum emplacement ages spanning approximately 2.80–2.71 Ga. The Elk Gulch Suite and Dillon Gneiss are difficult to differentiate in the field; the former tends to be more mafic and richer in plagioclase (Garihan, 1979b). The older gneissic sequences form the basement to the younger Christensen Ranch Metasedimentary Suite (James, 1990), which comprises a complex sequence of metasedimentary rock distinguished by intertonguing marble and schist intervals. Amphibolite (XAam) occurs as screens or sheets in all three metamorphic belts but was only mapped in areas thick and abundant enough to be shown at 1:24,000 scale. Archean ultramafic rock (XAum) occur as local intrusions in the older basement units and as large bodies composing the Wolf Creek plutonic complex in the northeast part of the map area. Northwest-striking diabase dikes generally crosscut the gneissic layering in the crystalline basement rocks and parallel northwest-striking fractures and faults. In the west-adjacent Ashbough Canyon 7.5' quadrangle, the Dillon Gneiss assemblage hosts graphite veins historically mined at the Crystal Graphite mine (Perry, 1948).

Yd **Diabase (Mesoproterozoic?)**—Diabase dikes that are approximately 1–30 m (3–100 ft) thick with continuous lengths exceeding 8.5 km (5.3 mi). A diabase body partially covered by a landslide in the north-central part of the map area is at least 250 m (820 ft) wide. Diabase is recessive and weathers to spheroidal boulders, commonly creating topographic sags. The rock is frequently altered to secondary minerals, but original diabasic and gabbroic textures are well preserved. Primary minerals appear to have been plagioclase and pyroxene, with minor amounts of quartz, magnetite, and ilmenite. Secondary minerals include actinolite, chlorite, and sericite. Wooden and others (1978) described the Ruby Range diabase as low potassium tholeiite with a whole-rock Rb-Sr age of 1.4 Ga. In the neighboring Tobacco Root Mountains, zircon isolated from a tholeiitic mafic dike yielded a ^{207}Pb/^{206}Pb of approximately 2.06 Ga (Mueller and others, 2004).

XAp **Pegmatite intrusions (Early Proterozoic (?) or Late Archean(?))**—Small pegmatite bodies (<30 m thick) intruding the Christensen Ranch Suite in the northern part of the quadrangle. Consists of coarse-grained alkali feldspar and quartz with minor amounts of albite–oligoclase and rare muscovite, tourmaline, and garnet. Most bodies show cataclastic deformation and are locally foliated.

XAam **Amphibolite (Archean or Early Proterozoic)**—Black and white, massive- to well-foliated, amphibolite composed of fine- to coarse-grained hornblende, plagioclase, and quartz. Typically occurs as two compositional varieties: gneiss containing 40–50 percent hornblende in alternating hornblende-rich and quartz–plagioclase-rich layers; or hornblendite with accessory plagioclase and quartz. The presence of garnet varies from approximately 0–25 percent. Amphibolite is intercalated with the other basement assemblages, ranging in size from centimeter-scale lenses to extensive sheets that are tens of meters thick.

XAum **Ultramafic rocks (Late Archean or Early Proterozoic)**—Intrusive bodies of ultramafic rock that typically occur as pods or lenses tens of meters wide, but form two plutons in the northeast part of the map area that exceed 2 km (1.25 mi) in length, including the Wolf Creek Pluton (Heinrich, 1960, 1963). Ultramafic rock is generally dark green or black, fine- to coarse-grained, and primarily massive to schistose. Weathering surfaces are commonly studded with resistant poikilitic orthopyroxene grains up to a few centimeters in diameter. The protolith composition likely ranged from harzburgite to pyroxenite, but most occurrences have been modified extensively by serpentinization and post-emplacement metamorphism.

XAcr **Christensen Ranch Metasedimentary Suite, undivided (Late Archean or Early Proterozoic)**—A complex sequence of marble, schist, and, quartzite that is intercalated with gneiss and amphibolite. Poor rock exposure made delineating the metasedimentary assemblages challenging, so they were mapped as a single unit. See James (1990) and Okuma (1971) for detailed mapping of the Christensen Ranch Metasedimentary Suite. Previous U-Pb monazite dating from schist, amphibolite, and gneiss yielded peak metamorphic ages spanning approximately 1.81–1.75 Ga (Jones, 2008; Cramer, 2015).

Marble (Late Archean to Early Proterozoic)—White, gray, orange-brown, medium- to coarsely crystalline dolomitic and calcitic marble that forms outcrops commonly covered with bright orange lichen. Marble contains light-colored diopside, tremolite, and scarce graphite; conspicuous dark green blebs of serpentine and phlogopite are characteristic of some intervals. Marble occurs as massive to well-foliated successions that appear conformable; however, the original stratigraphic order has likely been disrupted by bedding-plane faults and possible nappe development. In the northern part of the map area, marble layers are isoclinally folded into the older gneissic assemblages (Adg). Thicker intervals of pure marble are dominantly dolomitic in composition and commonly host talc deposits occurring as seams and pods. Structural thickness exceeds 400 m (1,313 ft).

Undifferentiated metasedimentary rocks (Late Archean or Early Proterozoic)—Complex sequence of quartz–mica schist and quartzose gneiss; calc–silicate gneiss and schist; and anthophyllite schist locally intercalated with amphibolite. Generally recessive and not exposed in the map area. Thickness unknown.

Adg **Dillon Gneiss (Archean)**—Gray to reddish brown, massive- to well-foliated, medium- to coarse-grained, locally garnetiferous gneiss of granitic composition that typically forms large, rounded outcrops. Potassium feldspar is the most abundant mineral, intergrown with oligoclase and quartz in nearly equal proportions. Subordinate mineral constituents include biotite, muscovite, garnet, and fibrous sillimanite. Massive to weakly foliated gneiss often grades into a strongly banded gneiss with a greater abundance of dark minerals, including biotite, garnet, and occasional hornblende. The Dillon Gneiss includes subordinate layers and pods of amphibolite, narrow ribbons of infolded marble, thin layers of pelitic gneisses and schists, and ultramafic rock. Originally named the "Dillon Granite Gneiss" (Heinrich, 1960) and subsequently referred to as "Quartzofeldspathic Gneiss" by James (1990). Stotter (2019) suggested the assemblage be renamed the "Dillon Gneiss," which is adopted in this map. U-Pb zircon data constrain minimum emplacement ages spanning between approximately 2.80 and 2.71 Ga (fig. 3).

Aeg **Elk Gulch Suite (Archean)**—Varied assemblage of biotite gneiss, hornblende gneiss, augen gneiss, migmatite, and amphibolite. The most abundant rock type is a banded migmatic gneiss composed of conspicuous dark layers of biotite and hornblende that alternate with layers consisting primarily of quartz and feldspar. Layers of pelitic schists and gneisses are common throughout the unit. The Elk Gulch Suite is generally more mafic and aluminous than the Dillon Gneiss. This unit was previously named the "pre-Cherry Creek Group" (Heinrich, 1960) and "Older Gneiss and Schist" (James, 1990). Stotter (2019) renamed the assemblage the Elk Gulch Suite after its type locality, which was adopted in this map. U-Pb zircon data constrain minimum emplacement ages between approximately 2.79 and 2.71 Ga (fig. 3).

STRUCTURAL GEOLOGY

Precambrian Deformation

Metamorphic foliations are generally parallel to compositional and migmatic layering (fig. 5A), and appears to be penetrative across the Elk Gulch Suite, Dillon Gneiss, and Christensen Ranch Suite assemblages. Widespread isoclinal folding is mostly axial planar to the main metamorphic foliation and readily visible in outcrops of the Dillon Gneiss assemblage. Most isoclinal folds plunge northeasterly, paralleling mineral and intersection lineations (fig. 5B). Parallel folds are the most common, and similar folds are observed locally. The primary metamorphic foliation is folded by an open and upright antiform–synform pair in the central map area. Several northwest-trending faults transect the quadrangle, including the Elk Gulch, Hoffman Gulch, and Carter Creek faults, all of which were active in Precambrian time with left-lateral displacements up to 2 km (1.25 mi) that occured before emplacement of the Proterozoic diabase dikes (Yd). The diabase dikes generally crosscut gneissic banding and intrude the Elk Gulch fault, constraining early deformation and metamorphism before approximately 2.1–1.4 Ga (Wooden and others, 1978; Mueller and others, 2004). Previously published geochronology ages (e.g., Harms and Baldwin, 2020; Jones, 2008; Cramer, 2015) and U-Pb zircon data from this study (fig. 3) record magmatic and tectonothermal pulses ca. 2.8–2.7 Ga; 2.5–2.4 Ga (Beaverhead/Tendoy orogeny); and 1.8–1.7 Ga (Big Sky orogeny).

Cordilleran Thrust Belt Deformation

Paleozoic–Mesozoic strata that unconformably rest on the crystalline basement in the northern Ruby Range are deformed by Late Cretaceous folds and faults (Tysdal, 1976; Parker and Gavillot, 2024; Gavillot and others, 2024). In the southern part of the range, the Phanerozoic cover was exhumed and completely eroded during crustal shortening, exposing the Precambrian basement rocks in the Elk Gulch quadrangle. Cordilleran structures were not readily identified in the map area, but the older northwest-striking Precambrian faults were possibly reactivated as contractional structures during crustal shortening. Low-temperature thermochronology data from the northern part of the Ruby Range suggest that rapid cooling and inferred tectonic exhumation of the basement rocks were underway by approximately 80 Ma (Carrapa and others, 2019).

Cenozoic Extensional Deformation

The Elk Gulch, Hoffman Gulch, and Carter Creek faults were extensively inverted during the Cenozoic and have remained active in the Quaternary (Schmidt and Garihan, 1983; Stickney and Bartholomew, 1987; James, 1990; Ostenaa and Wood, 1990). The Carter Creek and Hoffman faults are assumed to be the northwestern extent of the well-studied Sweetwater fault zone (fig. 1). In the adjacent Red Canyon 7.5' quadrangle, the Sweetwater fault displaces the Timberhill Basalt (ca. 6 Ma) down to the northeast approximately 200–250 m (655–820 ft; Stickney and Bartholomew, 1987; Ostenaa and Wood, 1990; Mosolf and Sears, 2024). Tertiary growth strata are preserved in the hanging wall and footwall of the fault, recording fault movement from the late Eocene to the Miocene. Using the Timber Hill Basalt as a structural datum, the Sweetwater fault's average slip rate from 6 Ma to the present is approximately 0.03–0.04 mm/yr (0.001–0.002 in/yr; Stickney and Bartholomew, 1987; Ostenaa and Wood, 1990; Fritz and Sears, 1993).

ACKNOWLEDGMENTS

Connie Thomson, Daniel Brennan, Stuart Parker, and Raymond Salazar performed mineral separations at the MBMG Mineral Separation Laboratory. Andrew Kylander-Clark supported LA-ICPMS analyses and data reduction at the University of California, Santa Barbara. Ashley and Arron Steiner directed bulk-rock geochemical analyses at the Washington State University Peter Hooper Geoanalytical Laboratory.

REFERENCES

Brennan, D.T., Parker, S., Mosolf, J.G., and Kylander-Clark, A., in review, U-Pb geochronology data from rock samples collected in western Montana, 2023–2024: Montana Bureau of Mines and Geology Analytical Dataset.
Carrapa, B., DeCelles, P.G., and Romero, M., 2019, Early inception of the Laramide orogeny in southwestern Montana and northern Wyoming: Implications for models of flat-slab subduction: Journal of Geophysical Research: Solid Earth, v. 124, p. 2102–2123.
Cramer, M., 2015, Proterozoic tectonometamorphic evolution of the Ruby Range, SW Montana, USA: Insights from phase equilibria modeling and in situ monazite petrochronology: Missoula, University of Montana, M.S. thesis, 120 p.
Dahl, P.S., 1979, Comparative geothermometry based on major-element and oxygen isotope distributions in Precambrian metamorphic rocks from southwestern Montana: American Mineralogist, v. 64, p. 1280–1293.
Dahl, P.S., 1980, The thermal-compositional dependence of Fe^{2+}–Mg distributions between coexisting garnet and pyroxene-applications to geothermometry: American Mineralogist, v. 65, p. 854–866.
Dahl, P.S., and Friberg, L.M., 1980, The occurrence and chemistry of epidote-clinozoisites in mafic gneisses from the Ruby Range, southwestern Montana: University of Wyoming Contributions to Geology, v. 18, no. 2, p. 77–82.
Desmarais, N.R., 1981, Metamorphosed Precambrian ultramafic rocks in the Ruby Range, Montana: Precambrian Research, v. 16, p. 67–101.
ESRI, 2024, "World_Imagery" [basemap], scale not given. "World Imagery Map," https://services.arcgisonline.com/ArcGIS/rest/services/World_Imagery/MapServer, accessed June 17th, 2024.
Fritz, W.J., and Sears, J.W., 1993, Tectonics of the Yellowstone hotspot wake in southwestern Montana: Geology, v. 21, p. 427–430.
Gavillot, Y.G., Parker, S.D., and Pearson, D.M., 2024, Geologic map of the Beaverhead Rock SE 7.5' quadrangle, Madison County, Montana: Montana Bureau of Mines and Geology Geologic Map 101, 1 sheet, scale 1:24,000, https://doi.org/10.59691/AKIR4686.
Garihan, J.M., 1979a, Geology and structure of the central Ruby Range, Madison County, Montana Summary: Geological Society of America Bulletin, Part I, v. 90, no. 4, p. 323–326.
Garihan, J.M., 1979b, Geology and structure of the central Ruby Range, Madison County, Montana: Geological Society of America Bulletin, Part II, v. 90, p. 695–788.
Harms, T.A., and Baldwin, J.A., 2020, Paleoproterozoic geology of Montana, *in* Metesh, J.J., and Vuke, S., eds.: Montana Bureau of Mines and Geology Special Publication 122: Geology of Montana—Geologic History, v. 1, 65 p., available at http://www.mbmg.mtech.edu/pubs/GeologyofMontana/
Heinrich, E.W., 1960, Geology of the Ruby Mountains and nearby areas in southwestern Montana, *in* Pre-Beltian geology of the Cherry Creek and Ruby Mountains areas, southwestern Montana: Montana Bureau of Mines and Geology Memoir 38, p. 31–62.
Heinrich, E.W., 1963, Paragenesis of clinohumite and associated minerals from Wolf Creek, Montana: American Mineralogist, v. 48, p. 597–613.
James, H.L., 1990, Precambrian geology and bedded iron deposits of the southwestern Ruby Range, Montana: U.S. Geological Survey Professional Paper, v. 1495, p. 1–39.
Jones, C.L., 2008, U-Pb geochronology of monazite and zircon in Precambrian metamorphic rocks from the Ruby Range, SW Montana: Deciphering geological events that shaped the NW Wyoming province: Kent, Kent State University, M.S. thesis, 119 p.
Karasevich, L.P., 1980, Structure of the pre-Beltian metamorphic rocks of the northern Ruby Range, southwestern Montana: Harrisburg, Pennsylvania State University, M.S. thesis, 172 p.
Klepper, M.R., 1950, Geologic reconnaissance of parts of Beaverhead and Madison counties, Montana: U.S. Geological Survey Bulletin 969-C, p. 55–85, scale 1:250,000.
Lane, E.W., 1947, Report of the subcommittee on sediment terminology: Transactions of the American Geophysical Union, v. 28, no. 6, p. 936–938.
Le Bas, M.J., and Streckeisen, A.L., 1991, The IUGS systematics of igneous rocks: Journal of the Geological Society of London, v. 148, p. 825–833.
Le Bas, M.J., Le Maitre, R.W., Streckeisen, A., and Zanettin, B., 1986, A chemical classification of volcanic rocks based on the total alkali silica diagram: Journal of Petrology, v. 27, p. 745–750.
Marvin, R.F., Wier, K.L., Mehnert, H.H., and Merritt, V., 1974, K-Ar ages of selected Tertiary igneous rocks in southwestern Montana: Isochron/West, v. 10, p. 17–20.
Monroe, J.S., 1976, Vertebrate paleontology, stratigraphy, and sedimentation of the upper Ruby River basin, Madison County, Montana: Missoula, University of Montana, Ph.D. dissertation, 301 p.
Mosolf, J.G., Parker, S., Brennan, D.T., and Gavillot, Y., in review, Major oxide and trace element analyses of rock samples collected in southwest Montana: Montana Bureau of Mines and Geology Analytical Dataset.
Mosolf, J.G., and Sears, J., 2024, Geologic map of the Red Canyon 7.5' quadrangle, Beaverhead and Madison counties, Montana: Montana Bureau of Mines and Geology Geologic Map 95, 1 sheet, scale 1:24,000.
Mosolf, J.G., and Kylander-Clark, A., 2023, U-Pb geochronology data from rock samples collected in the Dillon, Hamilton, Philipsburg, Townsend, and Wisdom 30' x 60' quadrangles, western Montana, 2020-2021: Montana Bureau of Mines and Geology Analytical Dataset 3, https://doi.org/10.59691/FIIS4859.
Mueller, P.A., Burger, R., Wooden, J.L., Heatherington, A.L., Mogk, D.W., and D'Arcy, K., 2004, Age and evolution of the Precambrian crust of the Tobacco Root Mountains, Montana: Geological Society of America Special Papers, p. 181–202.
Okuma, A.F., 1971, Structure of the Southwestern Ruby Range near Dillon, MT: Harrisburg, State College, Pennsylvania State University, Ph.D. dissertation, 122 p.
Ostenaa, D., and Wood, C., 1990, Seismotectonic study for Clark Canyon Dam, Pick-Sloan Missouri Basin Program, Montana: U.S. Bureau of Reclamation Seismotectonic Report 90-4, 78 p., 1 pl.
Parker, S.D., and Gavillot, Y.G., 2024, Geologic map of the Laurin Canyon 7.5' quadrangle, Madison County, Montana: Montana Bureau of Mines and Geology Geologic Map 98, 1 sheet, scale 1:24,000, https://doi.org/10.59691/WMJR3264.
Perkins, M.E., and Nash, B.P, 2002, Explosive silicic volcanism of the Yellowstone hotspot: The ash fall record: Geological Society of America Bulletin, v. 114, p. 367–381.
Perry, E.S., 1948, Talc, graphite, vermiculite and asbestos in Montana: Montana Bureau of Mines and Geology Memoir 27, 44 p.
Pierce, K.L., and Morgan, L.A., 1990, The track of the Yellowstone hotspot—Volcanism, faulting, and uplift: U.S. Geological Survey Open-File Report 90-415, 68 p., 1 pl.
Ruppel, E.T., O'Neill, J.M., and Lopez, D.A., 1993, Geologic map of the Dillon 1º x 2º quadrangle, Idaho and Montana: U.S. Geological Survey Miscellaneous Investigations Series Map I-1803-H, scale 1:250,000.
Schmid, R., Fettes, D., Harte, B., Davis, E., and Desmons, J. A., 2007, Systematic nomenclature for metamorphic rocks: 1. How to name a metamorphic rock. Recommendations by the IUGS Subcommission on the Systematics of Metamorphic Rocks, available at https://www.bgs.ac.uk [Accessed March 2023].
Schmidt, C.J., and Garihan, J.M., 1983, Laramide tectonic development of the Rocky Mountain foreland of southwestern Montana, *in* Lowell, J.D., and Gries, R., eds.: Rocky Mountain foreland basins and uplifts: Rocky Mountain Association of Geologists, p. 271–294.
Sears, J.W., Hendrix, M.S., Thomas, R.C., and Fritz, W.J., 2009, Stratigraphic record of the Yellowstone hotspot track, Neogene Sixmile Creek Formation grabens, southwest Montana: Journal of Volcanology and Geothermal Research, v. 188, p. 250–259.
Shane, P.A., and Sears, J.W., 1995, Miocene tephra beds in SW Montana: Geochronology, geochemistry and implications: Geological Society of America, Abstracts with Programs, v. 27, no. 4, p. 55.
Stickney, M.C., and Bartholomew, M.J., 1987, Seismicity and late Quaternary faulting of the northern Basin and Range province, Montana and Idaho: Bulletin of the Seismological Society of America, v. 77, p. 1602–1625.
Stotter, S.V., 2019, Determining the Precambrian structure and thermotectonic evolution of the central Ruby Range, southwest Montana: Missoula, University of Montana, M.S. thesis, 78 p.
Sun, S.S., and McDonough, W.F., 1989, Chemical and isotope systematics of oceanic basalts: Implications for mantle composition and processes, *in* Saunders, A.D., and Norry, M.J., eds., Magmatism in the ocean basins: Geological Society, London, Special Publications, v. 42, p. 313–345.
Thomas, R.C., and Sears, J.W., 2020, Middle Miocene through Pliocene sedimentation and tectonics in Montana: A record of the outbreak and passage of the Yellowstone Hotspot, *in* Metesh, J.J., and Vuke, S., eds.: Montana Bureau of Mines and Geology Special Publication 122: Geology of Montana—Geologic History, v. 1, 25 p., available at http://www.mbmg.mtech.edu/pubs/GeologyofMontana/
Thomas, R.C., Sears, W.S., Ripley, A.A., and Berg, R.B., 1995, Tertiary extensional history of southwestern Montana: Field trip guide for the Sweetwater and upper Ruby valleys, Montana: Northwest Geology, v. 25, p. 5–25.
Tysdal, R.G., 1976, Geologic map of the northern part of Ruby Range, Madison County, Montana: U.S. Geological Survey Miscellaneous Investigations Series Map I-951, scale 1:24,000.
Vuke, S.M., 2020, The Eocene through early Miocene sedimentary record in western Montana, *in* Metesh, J.J., and Vuke, S., eds.: Montana Bureau of Mines and Geology Special Publication 122: Geology of Montana—Geologic History, v. 1, 38 p., available at http://www.mbmg.mtech.edu/pubs/GeologyofMontana/
Vuke, S.M., Porter, K.W., Lonn, J.D., and Lopez, D.A., 2007, Geologic map of Montana: Montana Bureau of Mines and Geology Geologic Map 62, 73 p., 2 sheets, scale 1:500,000.
Wooden, J.L., Vitaliano, C.J., Koehler, S.W., and Ragland, P.C., 1978, The late Precambrian mafic dikes in the southern Tobacco Root Mountains, Montana Geochemistry, Rb-Sr geochronology, and

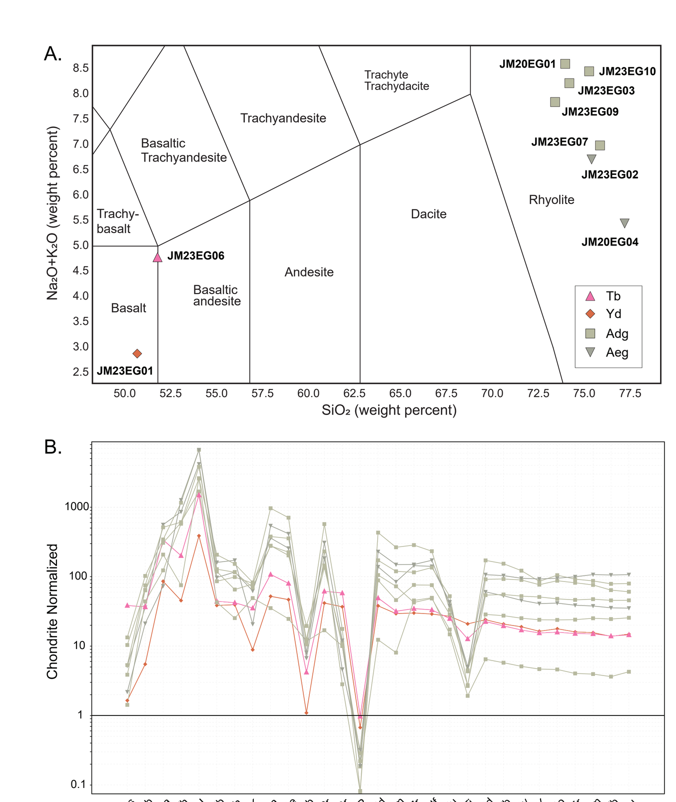

Figure 2. Whole-rock geochemical data. (A) Total alkali silica classification diagram of normalized values after Le Bas and others (1989). (B) Chondrite-normalized rare earth element plot after Sun and McDonough (1989). Data are color coded by unit; plots share the legend in (A).

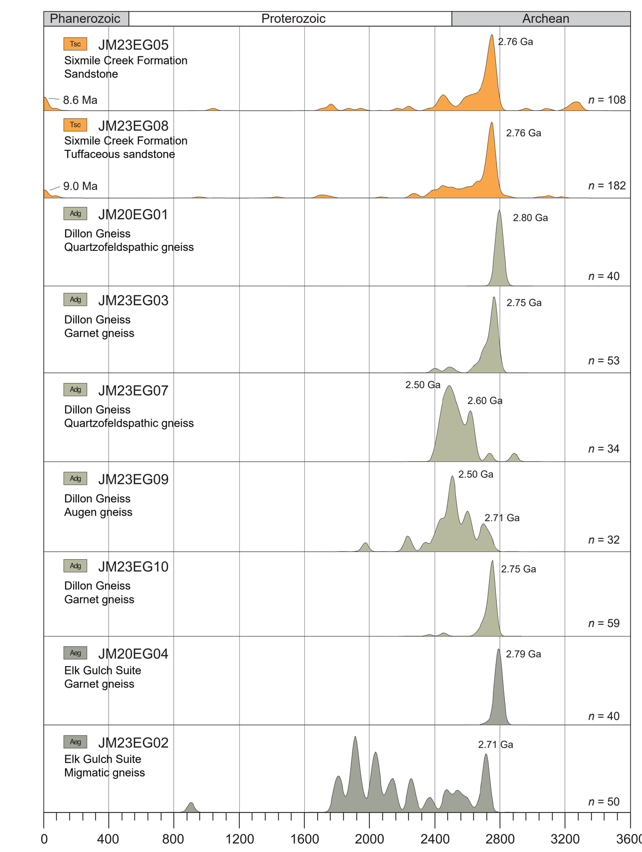

Figure 3. Kernel density estimate (KDE) plots of the ^{207}Pb corrected ^{206}Pb/^{238}U (<1,400 Ma) and ^{207}Pb/^{206}Pb (>1,400 Ma) zircon age data. KDE bandwidths and bin widths are 20 m.y. A 20 percent discordance filter was applied to the data. Major peak ages are labeled.

Figure 4. (A) Tertiary sediments of the Sixmile Creek Formation (Tsc) unconformably resting on Precambrian basement rocks, viewed from the Blacktail Deer Creek drainage south of the Sweetwater Hills. The Dillon Gneiss (Adg) forms the rocky skyline. Note the pediment surface formed on the Tertiary deposits. (B) Banded granitic gneiss forming blocky rock outcrops typical of the Dillon Gneiss unit (Adg).

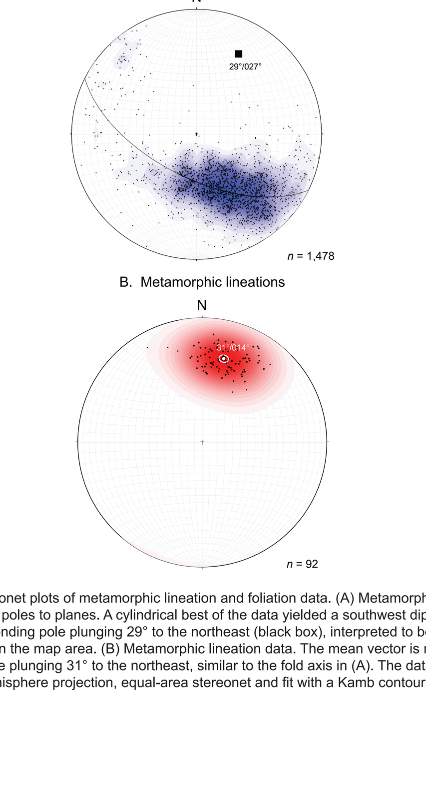

Figure 5. Stereonet plots of metamorphic lineation and foliation data. (A) Metamorphic foliation data plotted as poles to planes. A cylindrical best of the data yielded a southwest dipping plane with a corresponding pole plunging 29° to the northeast (black box), interpreted to be the general axis of folding in the map area. (B) Metamorphic lineation data. The mean vector is represented by a white circle plunging 31° to the northeast, similar to the fold axis in (A). The data are plotted on a lower-hemisphere projection, equal-area stereonet and fit with a Kamb contour.

Geologic Map 108

Geologic Map of the Elk Gulch 7.5′ Quadrangle, Southwestern Montana

Jesse G. Mosolf

2025

https://doi.org/10.59691/NHYS7628